SOH Estimation of LMO/NMC-based Electric Vehicle Lithium-Ion Batteries Using the Incremental Capacity Analysis Technique

Stroe, Daniel-Ioan; Schaltz, Erik

Published in:
Proceedings of the 2018 IEEE Energy Conversion Congress and Exposition (ECCE)

DOI (link to publication from Publisher):
10.1109/ECCE.2018.8557998

Publication date:
2018

Document Version
Accepted author manuscript, peer reviewed version

SOH Estimation of LMO/NMC-based Electric Vehicle Lithium-Ion Batteries Using the Incremental Capacity Analysis Technique

Daniel-Ioan Stroe
Department of Technology
Aalborg University
Aalborg, Denmark
dis@et.aau.dk

Erik Schaltz
Department of Technology
Aalborg University
Aalborg, Denmark
esc@et.aau.dk

***Abstract*—The implementation of an accurate but also low computational demanding state-of-health (SOH) estimation algorithm represents a key challenge for the battery management systems in electric vehicle (EV) applications. In this paper we investigate the suitability of the incremental capacity analysis (ICA) technique for estimating the capacity fade and subsequently the SOH of LMO/NMC-based EV Lithium-ion batteries. Based on ageing results collected during eleven months of testing, we were able to accurately relate the capacity fade of the studied batteries to the evolution of the voltage value, which corresponds to one of the incremental capacity (IC) valleys, obtained using the ICA technique.**

Keywords—Lithium-ion Battery, SOH Estimation, Electric Vehicle, Incremental Capacity Analysis.

I. INTRODUCTION

During long time utilization, the capacity and power capability of Lithium-ion (Li-ion) batteries are subjected to gradual degradation [1]. Thus, knowledge about the batteries' state-of-health (SOH) becomes critical in practical applications (as is the case of electric vehicles - EVs), in order to ensure a safe and reliable operation. Depending on the requirements of the application, the SOH can be related either to the battery capacity or to the battery internal resistance/power; for example in the case of an EV battery, the SOH is related to the capacity as the user is mainly interested in the driving range, which depends on the available battery capacity.

Different methods for Li-ion battery SOH estimation have been reported in the literature [2]. According to Berecibar et al., the SOH estimation methods can be divided into two groups [3]. The first group are using adaptive methods such as Kalman filters, neural networks or fuzzy logic to calculate the parameters of the Li-ion battery which are subjected to degradation. Most of the times, these methods are very accurate; nevertheless, they require a lot of computational power, which makes them less suitable for battery-management-system (BMS) implementation in practical applications [3]. The second group of SOH estimation methods relies on classical experimental techniques such as current pulses, coulomb counting or data maps; these methods have low computational demands and are suitable for BMS implementation, however, sometimes their accuracy is limited [3].

The SOH estimation method, which we proposed in this paper, belongs to the second group of methods and is based on the incremental capacity analysis (ICA) technique. For prooving the suitability of the proposed SOH estimation method, we have used Li-ion batteries, specially designed for EV applications, which were subjected to eleven months of ageing tests carried out at different conditions.

The remaining of the paper is organized as follows. The ICA technique is introduced in Section II. The experimental set up, introducing the Li-ion battery cells use in this work and the considered aging tests are presented in Section III. The aging results and the proposed method for battery SOH estimation based on the ICA technique are introduced in Section IV, while conclusions to the work are given in Section V.

II. INCREMENTAL CAPACITY ANALYSIS TECHNIQUE

The ICA technique was initially used to study the electrochemical behavior of Li-ion batteries; more specific, ICA can be applied to analyze the lithium intercalation process and the corresponding staging phenomenon [4], [5]. Consequently, many researchers used this technique to determine the ageing mechanisms, which cause the gradual capacity fade of Li-ion batteries. The ICA technique consists in differentiating the battery charging capacity against the battery voltage. In the obtained incremental capacity (IC) curve, the voltage plateaus of the charging voltage are transformed into clearly visible *dQ/dV* peaks (also referred as IC peaks) [6], as illustrated in Fig. 1.

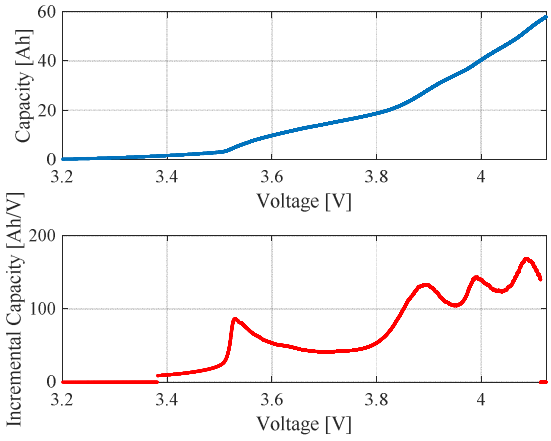

Fig. 1. Capacity (top) and IC (bottom) as a function of the battery voltage.

It is worth mentioning that in order to apply the ICA technique, the charging of the battery should take place with as low as possible current since a high current strongly influences the reactions in the cells and results into distorted or undetectable IC peaks. Furthermore, in order to allow for aging analysis and SOH estimation, the capacity measurement has to be performed with a consistently current and at the same temperature, since the ICA plots are very sensitive to the changes in both these parameters (i.e., current and temperature), as shown in Fig. 2. For example, a change from C/5 to C/2 in the charging current used during the capacity measurement can results in 15 % (i.e., 18.4 Ah/V) change in the amplitude of the IC peaks. Similarly, a shift in the measurement temperature, from 15 to 30 ºC, can results in approximatively 20 % (i.e., 26.2 Ah/V) deviation in the amplitude of IC peak.

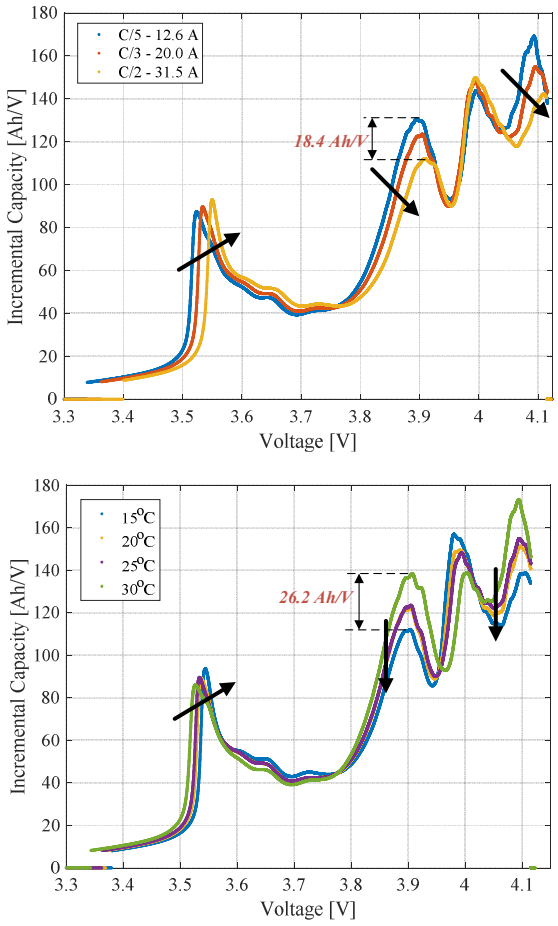

Fig. 2. Influence of the charging C-rate (top) and temperature (bottom) on the IC plot; the arrows highlight the increase on the C-rate (top) and decrease in the temperature (bottom)

III. Experiment Set-Up

A. Tested Battery Cell

In this research, prismatic Li-ion battery cells with a nominal capacity of 63 Ah and a nominal voltage of 3.75 V were used (see Fig. 1). The cells are based on a graphite anode and a mixture of LMO/NMC at the cathode, Furthermore, they are specially designed for EV applications.

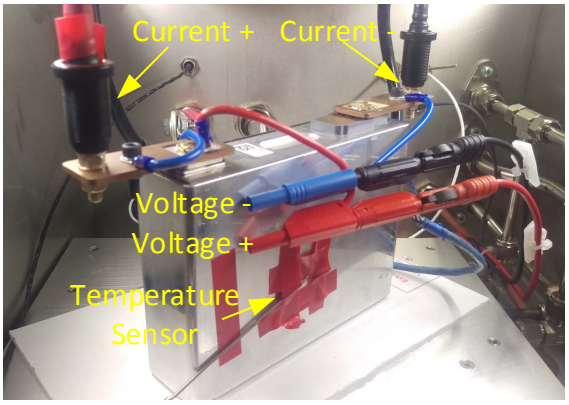

Fig. 3. LMO/NMC-based battery cell connected to the battery test station

B. Aging Conditions and Capacity Measurement

The performance (i.e., capacity and power) of Li-ion batteries are degrading during both cycle and calendar (e.g., stand-by) operation. However, there are many applications, where calendar ageing represents a high percentage of the battery operation during its life. For example, as it is presented in [7], batteries used in EVs spend approximately 90 to 95% of their lifetime in stand-by, which will cause calendar ageing. Furthermore, as shown by Swierczynski et al. in [8], more than 75% of the capacity fade to which a battery was subjected during EV operation was due to calendar ageing. Besides EVs, another application in which batteries will degrade due to idling are uninterruptable power systems, where the batteries are scarcely used as presented in [9]. Thus, we have considered that it is relevant to investigate the degradation and to estimate the SOH of Li-ion batteries, which are aged under calendar ageing conditions.

In order to consider different calendar ageing scenarios, a test matrix was developed and the considered LMO/NMC-based Li-ion batteries were aged at the conditions highlighted in Fig. 2. Each 30 days, the ageing tests were interrupted and a reference performance test (RPT) procedure was applied to the cells. Among various parameters, the capacity of the battery cells was measured during the RPT at a temperature of 25°C. In order to comply with the requirements of the ICA technique, which demands the capacity measurement with a small C-rate, the capacity of the LMO/NMC cells was measured with C/5 (i.e., 12.6 A) during both charging and discharging.

TABLE I. Calendar Aging Conditions for the LMO/NMC Battery Cells

SOC	Temperature			
	5 ºC	*35 ºC*	*45 ºC*	*45 ºC*
10 %				X
50 %	X	X	X	X
90 %				X

IV. Results

A. Capacity Fade

The LMO/NMC-based Li-ion battery cells were aged at the calendar conditions presented in Fig. 2 for a period of 210 days. For analyzing the effect of different ageing conditions on the battery capacity, the measured capacities

were normalized to the corresponding values measured at the beginning of life (BOL) according to (1). Fig. 3 and Fig. 4 present the effect on the battery capacity fade of storage temperature and storage SOC, respectively.

$$Capacity\ [\%] = Capacity_{actual} / Capacity_{BOL} \cdot 100\% \quad (1)$$

Where $Capacity_{actual}$ [Ah] represents the battery actual capacity measured during the ageing process and $Capacity_{BOL}$ [Ah] represents the battery capacity measured at the cells' BOL.

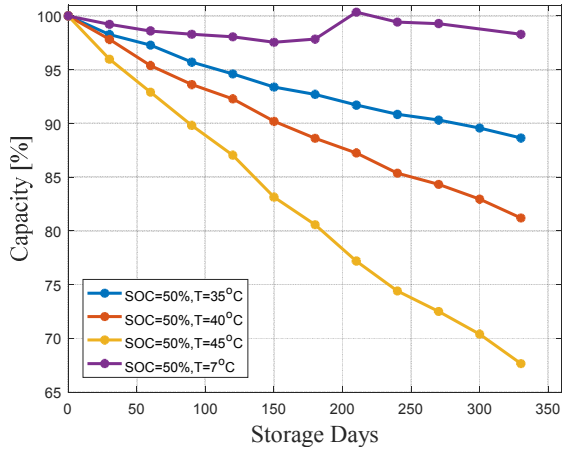

Fig. 4. Capacity fade of LMO/NMC-based battery cells measured at different temperatures and SOC = 50%.

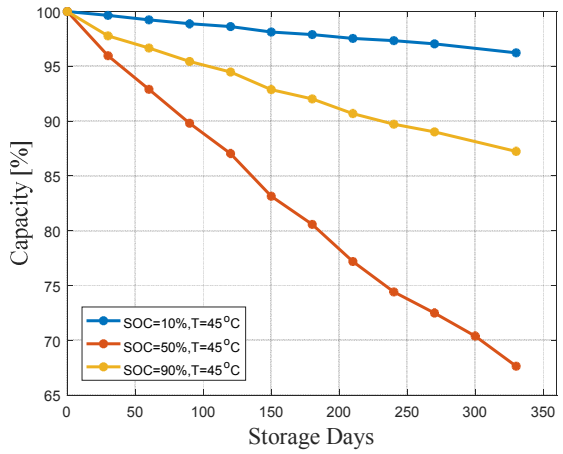

Fig. 5. Capacity fade of LMO/NMC-based battery cells measured at different SOCs and T = 45ºC.

As expected, the increase of the storage temperature causes the acceleration of the capacity fade; this behavior is especially obvious for the battery cell tested at 45°C, which during the seven months of ageing tests lost approximately 23% of its capacity, i.e. double than the battery cell tested at 40°C. These results are in good agreement with the behavior of NMC battery cells, which are reported for example in [10]. The influence of the storage SOC on the capacity fade of the tested LMO/NMC cells is more complex than the influence of the temperature. As it is illustrated in Fig. 4, higher capacity fade was obtained for the case when the cells were stored at a middle SOC (i.e., 50%) than for the cells stored at extreme SOCs (i.e., 10% and 90%). A similar behavior was reported by Keil and Jossen in [11] for a NCA-based Li-ion battery.

B. ICA for LMO/NMC cells

A typical ICA plot for the studied LMO/NMC-based Li-ion battery cell is presented in Fig. 4. In the figure, six zones in the voltage interval 3.3 V - 4.1 V are highlighted for further analysis. This six zones are defined by twelve metric points, representing four IC peaks, two IC valleys, and their corresponding six voltage values.

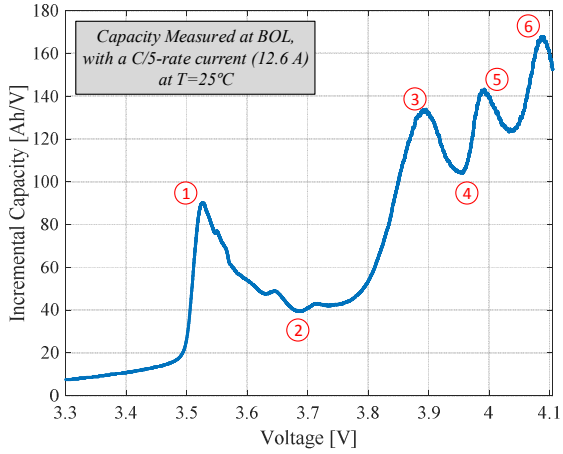

Fig. 6. ICA curve obtained for a C/5 charge of the LMO/NMC battery cells with five zones selected for further analysis.

The evolution of the ICA curves obtained during the calendar ageing process for the battery cell tested at 35°C and 50% SOC is presented in Fig. 5. By analyzing these results, obtained after 330 days of ageing, a-quasi monotonous displacement of the IC peaks and valleys in Zone 1, Zone 2, and Zone 4 was observed as illustrated in Fig. 8, Fig. 9, and Fig. 10, respectively. The evolutions of the IC peaks in Zone 3 and Zone 6 are scattered and no consistent ageing trends were observed. Furthermore, the IC peak corresponding to Zone 5 has ceased to be visible after 150 dyas of aging. Similar behaviors were obtained for the LMO/NMC battery cells aged at the other considered conditions. Therefore, the following analysis is focused only on the results obtained for the LMO/NMC battery cell aged at 35 ºC and 50% SOC.

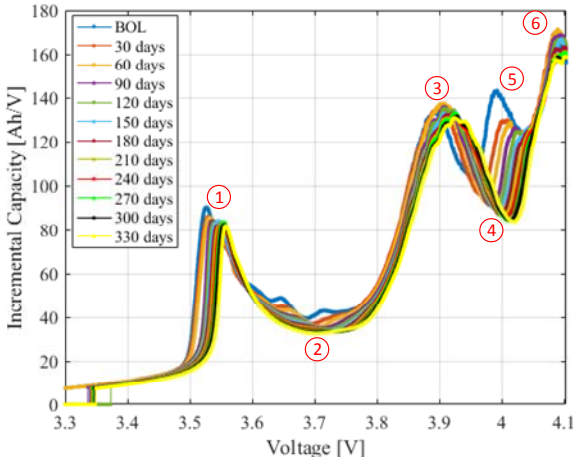

Fig. 7. Evolution of the ICA curve corresponding to the battery cell aged at T=35°C and SOC=50%.

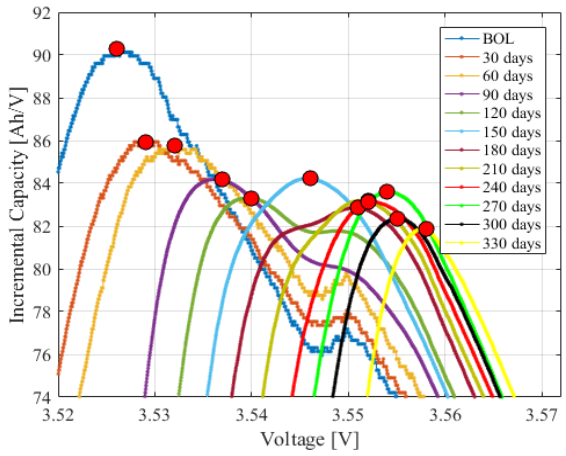

Fig. 8. Evolution of the IC peak in Zone 1 for the battery cell aged at T=35°C and SOC=50%.

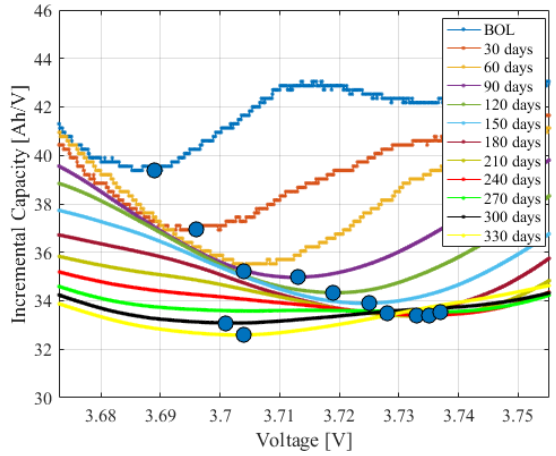

Fig. 9. Evolution of the IC valley in Zone 2 for the battery cell aged at T=35°C and SOC=50%.

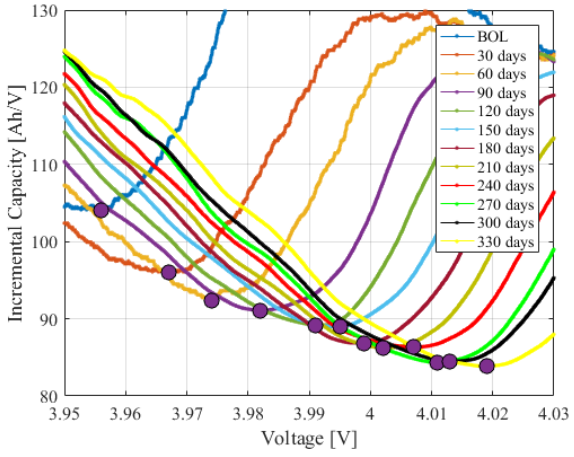

Fig. 10. Evolution of the IC valley in Zone 4 for the battery cell aged at T=35°C and SOC=50%.

C. *ICA-based SOH estimation*

The evolution of the peak and valleys and their corresponding voltage values, corresponding to Zone 1, Zone 2, and Zone 4 was further analyzed. Thus, based on (2), (3), and (4), we have related the values of the IC peaks and valleys and their corresponding voltage levels, obtained during aging, to the values, which were obtained at the battery cell BOL.

$$ICpeak_{\text{evolution}}\,[\%] = ICpeak_{\text{actual}} / ICpeak_{\text{BOL}} \cdot 100\% \quad (2)$$

$$ICvalley_{\text{evolution}}\,[\%] = ICvalley_{\text{actual}} / ICvalley_{\text{BOL}} \cdot 100\% \quad (3)$$

$$V_{\text{evolution}}\,[\%] = V_{\text{actual}} / V_{\text{BOL}} \cdot 100\% \quad (4)$$

Where $ICpeak_{\text{evolution}}$ represents the change in the value of the IC peak (corresponding to Zone 1) caused by ageing, $ICpeak_{\text{actual}}$ represents the actual value of the IC peak measured after each 30 days of aging, and $ICpeak_{\text{BOL}}$ represents the value of the IC peak at the battery cell's BOL. Analogical definitions are valid for $ICvalley_{\text{evolution}}$, $ICvalley_{\text{actual}}$, $ICvalley_{\text{BOL}}$, $V_{\text{evolution}}$, V_{actual}, and V_{BOL}.

The evolution of the investigated IC peak value, valleys and their corresponding voltage values, during calendar ageing, at T=35°C and SOC=50%, are presented in Fig. 11 – Fig. 16, respectively.

By analyzing the aging results presented in Fig. 11 – Fig. 16, it can be observed that the evolution of the IC peak value corresponding to Zone 1 (Fig. 11) and the evolution of the voltage value corresponding to Zone 2 (Fig. 15), are not following consistent trends. Namely, the evolution of the IC peak value corresponding to Zone 1 is not monotonous, while in the evolution of the voltage value corresponding to Zone 2 a sudden decrease after 270 days of aging takes place.

After comparing the capacity fade behavior of the LMO/NMC battery cell aged at T=35°C and SOC=50%, which is presented in Fig. 4, with the evolutions of IC metric points (e.g., peaks, valleys, voltage values), presented in Fig. 12 – Fig. 14 and Fig. 16, similar aging trends have be observed. Thus, we have plotted the battery cell capacity fade as function of the evolution of the IC metric points, which were obtained through the ICA. As presented in Fig. 17 and Fig. 18, a power law function (5) fits with high accuracy the relationship between the battery capacity fade and the evolution of the IC valleys corresponding to Zone 2 and Zone 4, respectively. Moreover, it was found out that a linear relationship (6) exists between the evolution of the voltage value corresponding to Zone 1 and Zone 4 and the capacity fade of the LMO/NMC battery cells, as shown in Fig. 19 and Fig. 20.

$$Cfade\,[\%] = a \cdot ICvalley_{\text{evolution}}{}^{b} \quad (5)$$

$$Cfade\,[\%] = c \cdot V_{\text{evolution}} \quad (6)$$

Where C_{fade} represents the measured capacity fade of the LMO/NMC-based Li-ion battery cell, a and b represent the coefficient and exponent of the power law fitting function, while c represents the coefficient of the linear fitting function.

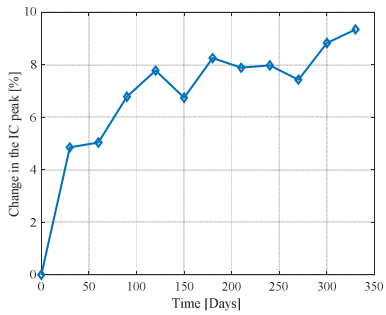

Fig. 11. Evolution during calendar aging of the IC peak value corresponding to Zone 1.

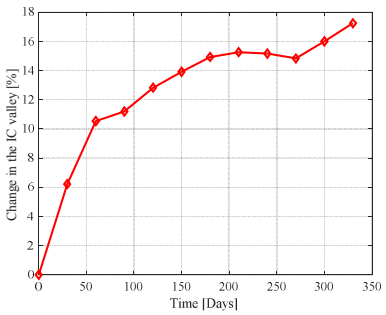

Fig. 12. Evolution during calendar aging of the IC valley value corresponding to Zone 2.

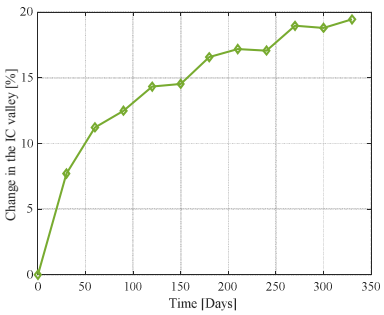

Fig. 13. Evolution during calendar aging of the IC valley value corresponding to Zone 4.

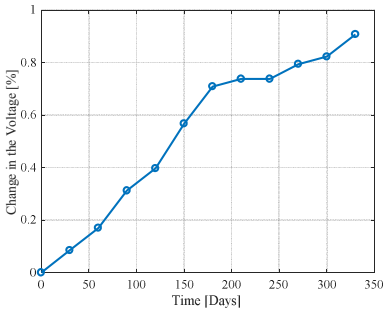

Fig. 14. Evolution during calendar aging of the voltage value corresponding to Zone 1.

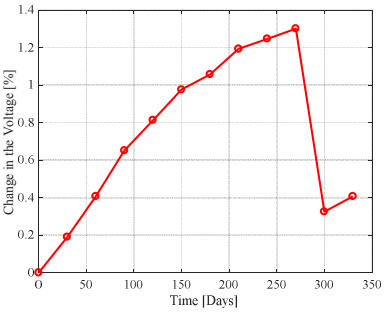

Fig. 15. Evolution during calendar aging of the voltage value corresponding to Zone 2.

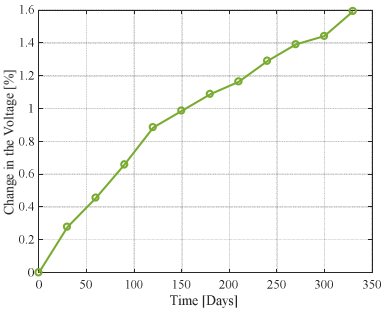

Fig. 16. Evolution during calendar aging of the voltage value corresponding to Zone 4.

Based on the results obtained from the fitting processes, it can be concluded that the capacity fade of the tested battery cells can be estimated most accurately by monitoring the evolution of the voltage value corresponding to the Zone 4, obtained by the ICA technique. In many applications (e.g., EVs, renewable energy storage), the capacity fade of the battery is directly used to express its SOH. Subsequently, based on the results presented in this section, the evolution of the voltage value corresponding to Zone 4 represents a very accurate and promising alternative to express the SOH of the studied LMO/NMC battery cell. Thus, in order to determine the battery's SOH, the lengthy capacity measurement (carried out over the entire battery voltage interval) can be replaced by a short charge of the battery in the interval 3.95 V – 4.05 V (the zone where the targeted IC valley appears) and the application of the ICA technique.

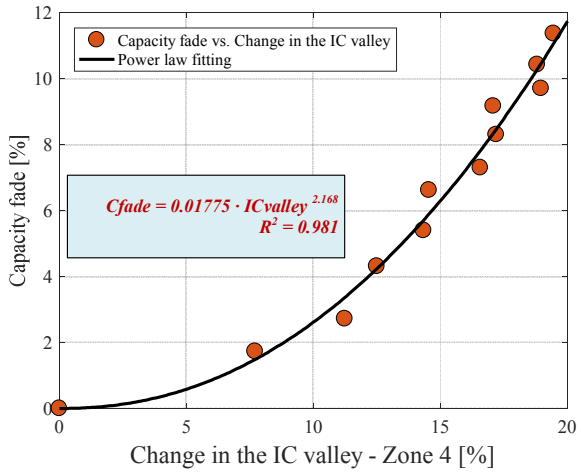

Fig. 17. Relationship betwe the battery capacity fade based and the IC valley evolution, corresponding to Zone 2.

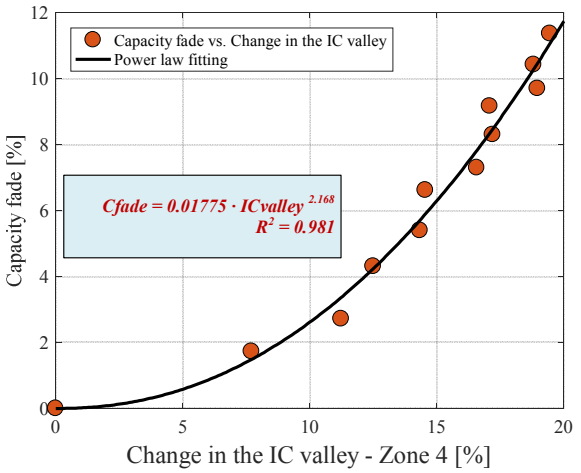

Fig. 18. Relationship betwe the battery capacity fade based and the IC valley evolution, corresponding to Zone 4.

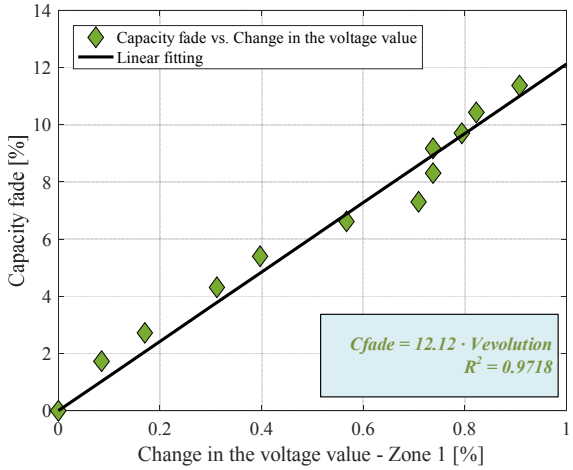

Fig. 19. Relationship betwe the battery capacity fade based and the voltage evolution, corresponding to Zone 1.

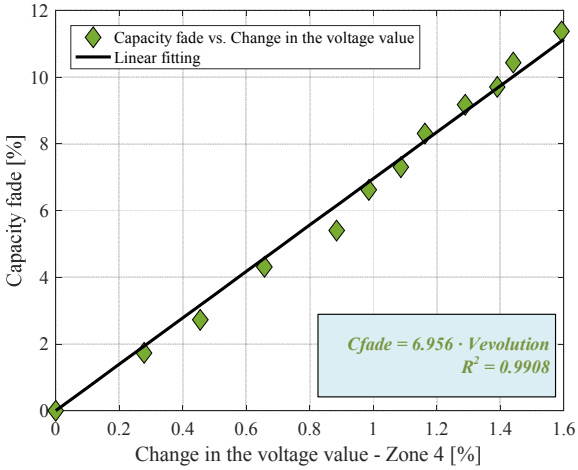

Fig. 20. Relationship betwe the battery capacity fade based and the voltage evolution, corresponding to Zone 4.

V. CONCLUSIONS

In this paper, it was shown that the ICA technique represents a reliable method for estimating the capacity fade, and subsequently the SOH of Li-ion batteries. Based on results from eleven months of calendar aging test at 35ºC and 50% SOC, we have been able to relate the capacity fade of a LMO/NMC-based EV Li-ion battery to various peaks and valleys and their corresponding voltage values, which were obtained by applying the ICA technique.

The IC plot of the studied LMO/NMC-based battery cells are described by six different zones, which correspond to twelve metric points. Out of the twelve metric points, only four, have shown consistent aging trends during calendar aging at 35ºC and 50% SOC. By relating thess four metric points with the measured battery capacity fade, it was found that evolution of the voltage value, corresponding to the valley in Zone 4, could estimate with very high accuracy the capacity fade and subsequently, the SOH of the studied LMO/NMC battery cells. In order to generalize this conclusion and to prove the applicability of the ICA technique for battery SOH estimation, the same analysis will be performed for the other battery cells aged at different conditions.

ACKNOWLEDGMENT

This work has been part of the Adaptive Battery Diagnostic Tools for Lifetime Assessment of EV batteries (BATNOSTIC) research and development project, project no. 64015-0611. The authors gratefully acknowledge EUDP Denmark for providing the financial support necessary for carrying out this work.

REFERENCES

[1] D.-I. Stroe et al., "Accelerated Lifetime testing methodology for Lifetime Estimation of Lithium-Ion batteries Used in Augmented Wind Power Plants," *IEEE Transactions on Industry Applications*, vol. 50, no. 6, pp. 4006-4017, Apr. 2014.

[2] W. Waag, C. Fleischer, D.U. Sauer, "Critical review of the methods for monitoring of lithium-ion batteries in electric and hybrid vehicles," *Journal of Power Sources*, vol. 258, pp. 321-339, 2014.

[3] M. Berecibar et al., "Critical review of state of health estimation methods of Li-ion batteries for real applications," *Renewable and Sustainable Energy Reviews*, vol. 56, pp. 572-587, 2016.

[4] J. Groot, "State-of-Health Estimation of Li-ion Batteries: Ageing Models," *Ph.D. Thesis*, Chalmers University of Technology, Göteborg, 2014.

[5] C. Weng, et al, "On-board state of health monitoring of lithium-ion batteries using incremental capacity analysis with support vector regression," *Journal of Power Sources*, vol. 235, pp. 36-44, 2013.

[6] M. Dubarry, V. Svoboda, R. Hwu, B. Y. Liaw, "Incremental Capacity Analysis and Close-to-Equilibrium OCV Measurements to Quantify Capacity Fade in Commercial Rechargeable Lithium Batteries," *Electrochemical and Solid-State Letters*, vol. 9, no.10, pp. A454-A457, 2006.

[7] A. Eddahech et al., "Remaining useful life prediction of lithium batteries in calendar ageing for automotive applications," *Microelectronics Reliability,* vol. 52, pp. 2438-2442, Sep. 2012.

[8] M. Swierczynski et al., "Suitability of the Nanophosphate LiFePO4/C Battery Chemistry for the Fully Electric Vehicle: Lifetime Perspective," *IEEE Transactions on Industry Applications*, vol. 51, no. 4, pp. 1-8, Mar. 2014.

[9] A. I. Stan et al., "A Comparative Study of Lithium Ion to Lead Acid Batteries for use in UPS Applications," in *IEEE 2014 International Telecommunications Energy Conference,* 2014, pp. 1-8.

[10] S. Käbitz et al., "Cycle and calendar life study on a graphite/ LiNi1/3Mn1/3Co1/3O2 high energy system. Part A: Full cell characterization," *Journal of Power Sources*, vol. 239, pp. 572-583, 2013.

[11] P. Keil and A. Jossen, "Calendar Aging of NCA Lithium-Ion Batteries Investigated by Differential Voltage Analysis and Coulomb Tracking," *Journal of The Electrochemical Society*, vol. 164, no. 1, pp. A6066-A6074, 2017.